

# Rapid acquisition of *in vivo* biological images by use of optical coherence tomography

G. J. Tearney, B. E. Bouma, S. A. Boppart, and B. Golubovic

Department of Electrical Engineering and Computer Science, Research Laboratory of Electronics,  
Massachusetts Institute of Technology, Cambridge, Massachusetts 02139

E. A. Swanson

Lincoln Laboratory, Massachusetts Institute of Technology, Lexington, Massachusetts 02173

J. G. Fujimoto

Department of Electrical Engineering and Computer Science, Research Laboratory of Electronics,  
Massachusetts Institute of Technology, Cambridge, Massachusetts 02139

Received March 13, 1996

The development of techniques for high-speed image acquisition in optical coherence tomography (OCT) systems is essential for suppressing motion artifacts when one is imaging living systems. We describe a new OCT system for performing micrometer-scale, cross-sectional optical imaging at four images/s. To achieve OCT image-acquisition times of less than 1 s, we use a piezoelectric fiber stretcher to vary the reference arm delay. A Kerr-lens mode-locked chromium-doped forsterite laser is employed as the low-coherence source for the high-speed OCT system. Dynamic, motion-artifact-free *in vivo* imaging of a beating *Xenopus laevis* (African frog) heart is demonstrated. © 1996 Optical Society of America

Optical coherence tomography (OCT) is a micrometer-scale cross-sectional optical imaging technique that uses low-coherence interferometry to obtain high-resolution images of microstructure in biological systems.<sup>1</sup> OCT has been extensively applied in ophthalmology, and clinical studies have shown that OCT can be used to diagnose a wide range of retinal macular diseases.<sup>2,3</sup> Recent studies have shown that OCT can image architectural morphology in highly optically scattering tissues such as skin,<sup>4</sup> the vascular system,<sup>5,6</sup> the gastrointestinal tract,<sup>7</sup> and developing embryos.<sup>8</sup> Because the resolution of OCT is an order of magnitude greater than that of other currently available cross-sectional imaging technologies, it provides information on the microstructure of biological specimens that previously could be obtained only with conventional excisional biopsy. The potential capability of OCT to perform optical biopsy, or non-invasive optical diagnostic imaging of *in vivo* tissue architectural morphology, has motivated advances in OCT technology that will permit *in vivo* diagnostic imaging. In this Letter we describe the development of high-speed OCT technology. High-speed image acquisition is essential for enabling motion-artifact-free imaging in living subjects to be performed.

OCT performs optical ranging in tissue by use of a fiber-optic Michelson interferometer with a low-coherence illuminating source. Because interference is observed only when the optical path lengths of the sample and the reference arms match to within the coherence length of the source, precision distance measurements are possible if the source has a short coherence length. One obtains the amplitude of reflected light as a function of depth within tissue by moving the reference arm of the interferometer at a constant velocity and filtering the interference fringes at the Doppler

frequency with a bandpass filter. The filtered signal is then demodulated and digitized. The result is the measurement of optical backscatter or reflectance versus axial range. A cross-sectional image is produced when sequential axial reflectance profiles are recorded while the beam position is scanned across the sample.

Currently, typical OCT systems used to study *in vitro* human tissue are implemented by use of superluminescent diodes (SLD's) with center wavelengths of 850 or 1300 nm.<sup>4-8</sup> The optical power available from SLD sources is limited. SLD-based OCT systems at 1300 nm have a free-space axial resolution of 15–40  $\mu\text{m}$ , a sample arm power of 50–150  $\mu\text{W}$ , and signal-to-noise ratios (SNR's) ranging from 90 to 110 dB.<sup>4-8</sup> *In vivo* OCT imaging with these systems would be exceedingly difficult because the image-acquisition times of these systems (10–60 s) cannot prevent motion artifacts. To achieve image-acquisition times of less than 1 s, an alternative to mechanical reference arm mirror translation must be developed. In addition, because a high SNR is necessary for imaging to significant depths within turbid media, any increase in image-acquisition rate must be accompanied by a commensurate increase in source optical power. In this Letter we present a new high-speed OCT system that addresses both of these concerns and achieves an acquisition rate of four images per second. The capabilities of this system are demonstrated by the motion-artifact-free, *in vivo* imaging of a *Xenopus laevis* (African frog) heart.

Previous OCT systems utilized a mechanically translated reference arm mirror to perform axial scanning. The mirror velocity for these systems was typically in the range of 30 mm/s, corresponding

to a Doppler frequency of 46 kHz at 1300 nm. For image-acquisition rates of four frames/s, the Doppler frequency must be increased by  $\sim 2$  orders of magnitude to 5 MHz. This would necessitate a reference mirror velocity of 3 m/s. Moreover, this velocity must be held constant for distances greater than a few millimeters and repetition rates of  $\sim 500$  Hz.

Because to our knowledge no cost-effective mechanical translator meeting these specifications is currently available, we have used an alternative technology based on piezoelectric transducers to induce stretch in an optical fiber.<sup>7,9</sup> As depicted in Fig. 1, a 40-m length of single-mode optical fiber was wrapped under constant tension around a PZM. Approximately 300 windings were used. A triangle wave tailored to minimize hysteresis inherent in the PZM was used to drive the modulator at a frequency of 600 Hz. The fiber was stretched as the PZM expanded, inducing a temporal delay on the light propagating within it. Multiple wraps of the long length of fiber allowed the small expansion of the PZM to be magnified to an optical path length delay of  $\sim 3$  mm.

Interferometric detection requires that the polarization states returned from both arms of the interferometer be identical. We have identified three separate impediments to maintaining balance in the returned polarizations: static polarization mismatch that is inherent in wrapping the fiber around the PZM, slow drift that results from frictional heating of the piezoelectric transducers, and fast modulation (within each scan) that results from applying a voltage to the reference arm PZM. Each of these effects must be either canceled within the interferometer arm in which it is induced or identically balanced in the other interferometer arm. We chose to match the static birefringence in the reference arm by wrapping a duplicate PZM with an identical length of fiber and inserting it into the sample arm.<sup>9</sup> The duplicate PZM was not modulated. We canceled the slow drift by controlling the temperature of the driven PZM in the reference arm. Finally, we canceled the dynamic birefringence modulation occurring during each scan of the reference arm PZM by inserting a Faraday rotator into the free-space region of each interferometer arm.<sup>10</sup> We note that the polarization conjugation performed by the Faraday rotators also contributed to improving small imperfections in both static polarization matching and thermal-drift cancellation. All three of these corrective mechanisms were necessary to provide complete polarization matching over the entire laser spectrum and collectively resulted in nearly 100% fringe contrast.

An additional technology necessary for producing a high-speed OCT system is a high-power, single-mode, low-coherence source. To maintain a useful imaging penetration depth in multiply scattering tissues (2–3 mm), the SNR of the OCT system must be greater than 100 dB. We measure the SNR experimentally by comparing the signal from a 100% reflector (mirror) with the variance of the signal with the sample arm blocked. For shot-noise-limited detection,

the SNR is proportional to the power incident upon the sample and inversely proportional to the signal bandwidth.<sup>11</sup> Because the bandwidth increases with scanning velocity, the power incident upon the sample must be increased commensurately with the increase in scanning speed to preserve the SNR.

Commercially available SLD's coupled to single-mode fibers are typically limited to output powers of  $\leq 1$  mW. Mode-locked solid-state lasers, however, are capable of delivering hundreds of milliwatts of short-coherence-length light with a single transverse spatial mode, which is ideal for coupling to optical fiber. A Kerr-lens mode-locked titanium-doped sapphire laser operating at 820 nm has already been demonstrated as a high-resolution source for OCT.<sup>12</sup> Although this laser source would be appropriate for fast-scanning OCT, previous investigations showed that imaging in human tissues with a source wavelength of 1300 nm permits significantly deeper image penetration than does imaging at 820 nm.<sup>6</sup> To achieve this wavelength range, we employed a Kerr-lens mode-locked chromium-doped forsterite laser.<sup>13,14</sup> Here the Cr:forsterite laser was set to produce 200 mW of single-mode output power with a bandwidth of 50 nm centered at 1290 nm. The free-space axial resolution, or coherence length, of the Cr:forsterite source coupled into the fast-scanning OCT system was  $15 \mu\text{m}$ . For actual measurements, the laser power was attenuated to 30 mW. The power incident upon the sample was 2 mW, providing a measured SNR of 112 dB.

The image-acquisition rate of the fast-scanning OCT system is sufficient to permit motion-artifact-free imaging of *in vivo* biological specimens. Figure 2 demonstrates this, showing images of the beating heart of an *in vivo* embryonic *Xenopus laevis* (African frog) taken with both a SLD-based mechanical scanning OCT system and the high-speed OCT system.

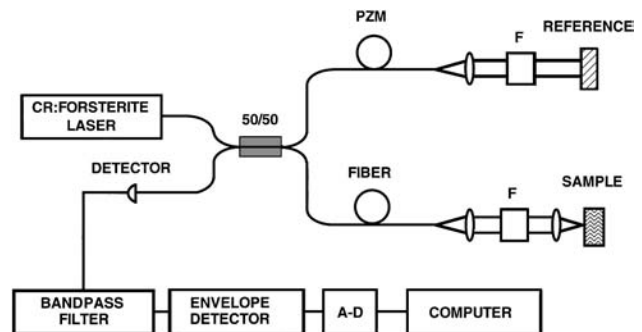


Fig. 1. Schematic of the high-speed OCT system. A Kerr-lens mode-locked Cr:forsterite laser is coupled into a fiber-optic Michelson interferometer. 40 m of single-mode optical fiber wrapped around a piezoelectric modulator (PZM) is placed in the reference arm. A matching length of fiber wrapped around a duplicate PZM is placed in the sample arm. Faraday rotators (F's) are used to compensate for bending-induced birefringence. Reflectivity as a function of depth is obtained by application of a triangle waveform to the reference arm PZM and demodulation of the resulting interference. An image is obtained by acquisition of reflectivity as a function of depth from within the sample while the sample arm beam is scanned across the specimen with a galvanometer mirror. A-D, analog-digital.

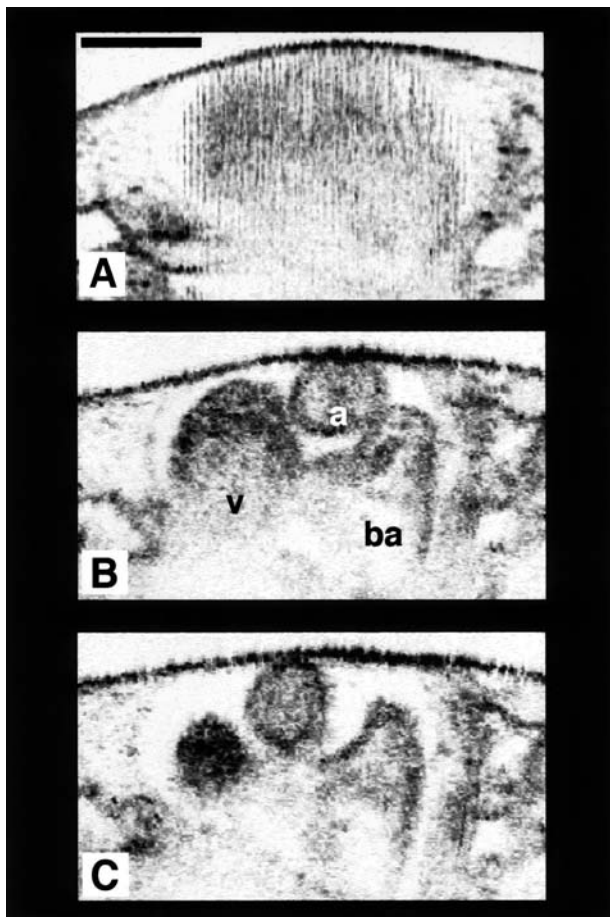


Fig. 2. A, OCT image of an *in vivo* *Xenopus laevis* (African frog) heart taken with a 1300-nm mechanical scanning SLD-based OCT system. The image-acquisition time was 30 s. The atrium (a) and the ventricle (v) are blurred owing to motion. B, High-speed OCT image permits visualization of the *in vivo* *Xenopus laevis* atrium (a), ventricle (v), and bulbus arteriosus (ba) during diastole. C, High-speed OCT image of the *in vivo* *Xenopus laevis* heart during systole. The image-acquisition times for B and C were 250 ms. The black bar in A represents 500  $\mu\text{m}$ .

The heart was imaged through the skin of the ventral side of the frog. Each image consists of  $300 \times 250$  pixels covering a sample area of  $3 \text{ mm} \times 2.2 \text{ mm}$ . The images were cropped and enlarged to display structures of interest. The focused transverse spot size was  $33 \mu\text{m}$ , corresponding to a confocal parameter of 1.34 mm. The SLD-based mechanical scanning OCT image was acquired in 30 s, and the high-speed OCT image was collected in 250 ms. The mechanical scanning OCT image of the heart is blurred owing to motion artifacts. These artifacts can be seen as vertical striations in the OCT image (Fig. 2A). The images acquired by the fast-scanning OCT system, however, show clear delineation of the anatomy of the heart, including atrium, ventricle, and bulbus arteriosus (Fig. 2B). In addition, the high-speed OCT system permits imaging of different stages of the cardiac cycle, such as diastole (ventricular relaxation and filling; Fig. 2B) and systole (ventricular contraction; Fig. 2C). Not only are these fast-scanning OCT

images motion artifact free but also they demonstrate the capability of high-speed OCT to permit the visualization of micrometer-scale anatomical function of *in vivo* biological specimens.

In conclusion, we have presented a fast-scanning OCT system capable of *in vivo* imaging of biological systems without image degradation owing to the motion of the specimen. The system integrates a PZM-driven optical fiber delay line and a high-power, short-coherence-length, mode-locked solid-state laser source. We acquired  $3 \text{ mm} \times 2.2 \text{ mm}$  images consisting of  $300 \times 250$  pixels at a rate of four images/s, with an axial resolution of  $15 \mu\text{m}$  and a SNR of 112 dB. The research presented here is an essential step toward enabling OCT to become a powerful tool for performing *in vivo* nonexcisional optical biopsy of human and other biological tissues.

This research is supported in part by National Institutes of Health contract NIH-9-RO1-EY11289-10, the Medical Free Electron Laser Program, U.S. Office of Naval Research contract N00014-94-1-0717, and U.S. Air Force Office of Scientific Research contract F49620-95-1-0221. We gratefully acknowledge fruitful scientific discussions with E. P. Ippen.

## References

1. D. Huang, E. A. Swanson, C. P. Lin, J. S. Schuman, W. G. Stinson, W. Chang, M. R. Hee, T. Flotte, K. Gregory, C. A. Puliafito, and J. G. Fujimoto, *Science* **254**, 1178 (1991).
2. M. R. Hee, J. A. Izatt, E. A. Swanson, D. Huang, C. P. Lin, J. S. Schuman, C. A. Puliafito, and J. G. Fujimoto, *Arch. Ophthalmol.* **113**, 325 (1995).
3. C. A. Puliafito, M. R. Hee, C. P. Lin, E. Reichel, J. S. Schuman, J. S. Duker, J. A. Izatt, E. A. Swanson, and J. G. Fujimoto, *Ophthalmology* **102**, 217 (1995).
4. J. M. Schmitt, M. Yablowsky, and R. F. Bonner, *Dermatology* **191**, 93 (1995).
5. J. G. Fujimoto, M. E. Brezinski, G. J. Tearney, S. A. Boppart, B. Bouma, M. R. Hee, J. F. Southern, and E. A. Swanson, *Nature Med.* **1**, 972 (1995).
6. M. E. Brezinski, G. J. Tearney, B. E. Bouma, J. A. Izatt, M. R. Hee, E. A. Swanson, J. F. Southern, and J. G. Fujimoto, *Circulation* **93**, 1206 (1996).
7. A. Sergeev, V. Gelikonov, G. Gelikonov, F. Feldchtein, K. Pravdenko, R. Kuranov, N. Gladkova, V. Pochinko, G. Petrova, and N. Nikulin, in *Conference on Lasers and Electro Optics '95*, Vol. 15 of 1995 OSA Technical Digest Series (Optical Society of America, Washington, D.C., 1995), paper CThN4.
8. S. A. Boppart, M. E. Brezinski, B. Bouma, G. J. Tearney, and J. G. Fujimoto, **177**, 54 (1996).
9. D. G. Luke, R. McBride, and J. D. C. Jones, *Opt. Lett.* **20**, 2550 (1995).
10. L. A. Ferreira, J. L. Santos, and F. Farahi, *Opt. Commun.* **114**, 386 (1995).
11. E. A. Swanson, D. Huang, and M. R. Hee, *Opt. Lett.* **17**, 151 (1992).
12. B. Bouma, G. J. Tearney, S. A. Boppart, M. R. Hee, M. E. Brezinski, and J. G. Fujimoto, *Opt. Lett.* **20**, 1486 (1995).
13. A. Seas, V. Petricevic, and R. R. Alfano, *Opt. Lett.* **17**, 937 (1992).
14. T. Carrig and C. R. Pollock, *IEEE J. Quantum Electron.* **29**, 2835 (1993).